Hindawi Publishing Corporation
Advances in Condensed Matter Physics
Volume 2013, Article ID 858406, 9 pages
http://dx.doi.org/10.1155/2013/858406

Research Article

Dielectric Properties of Φ(BZT-BCT)-(1−Φ) Epoxy Composites with 0-3 Connectivity

P. Mishra and P. Kumar

Department of Physics, National Institute of Technology, Rourkela 769008, India

Correspondence should be addressed to P. Kumar; pvn772004@yahoo.co.in

Received 30 May 2013; Revised 11 September 2013; Accepted 28 September 2013

Academic Editor: Mohindar S. Seehra

Lead free ferroelectric ceramic $[0.5[Ba(Zr_{0.2}Ti_{0.8})O_3]$-$0.5[(Ba_{0.7}Ca_{0.3})TiO_3]]$/(BZT-BCT)-epoxy composites with 0-3 connectivity (particles connected in 3 dimensions) were prepared using hand lay-up technique followed by cold pressing for different volume fractions of (BZT-BCT) ceramic powder in the epoxy polymer matrix. The structural, microstructural, and dielectric properties of the composites have been investigated and discussed. XRD studies revealed the presence of both ceramic and polymer phases in the (BZT-BCT)-epoxy composites. SEM studies showed a uniform distribution of ceramic particles in the epoxy matrix, which confirmed the 0-3 connectivity in the composites. Dielectric studies revealed an increase in relative permittivity (ε_r) and decrease in dielectric loss ($\tan\delta$) in the composites with the increase in the volume fractions of the ceramics up to 20%. This can be ascribed to the increase in density of the composites and dielectric properties of the epoxy polymer. At room temperature (RT) and at 1 kHz frequency, 0.2(BZT-BCT)-0.8(epoxy) composite showed the highest relative permittivity (ε_r) ~ 34. For the prediction of the effective dielectric constant of the composites, the experimental data were fitted to several theoretical equations. Effective medium theory (EMT) model and Yamada models were found to be useful for the prediction of the effective dielectric constant of studied composites.

1. Introduction

Lead based ferroelectric ceramics have been at the forefront of ceramic industry since decades. This is due to their excellent dielectric, piezoelectric properties and electromechanical coupling coefficients [1–5]. Apart from these properties, one of the most interesting and important properties of lead based materials is the presence of morphotropic phase boundary (MPB). MPB plays a crucial role in these systems in the enhancement of dielectric, piezoelectric, and electromechanical properties [1, 2, 6]. As a result, lead based ceramics are the mainstay for high performance piezoelectric actuators, ultrasonic transducers, sensors, and so forth [7–9]. Despite all its advantages, Pb based ceramics are facing global restrictions due to their toxicity [10]. Recently, the focus of study is on lead free ferroelectric ceramics. Liu et al. first reported a lead free pseudo-binary $x[Ba(Zr_{0.2}Ti_{0.8})O_3]$-$(1-x)[(Ba_{0.7}Ca_{0.3})TiO_3]$/(BZT-BCT) ferroelectric system to replace lead zirconate titanate (PZT) based systems [11]. This system possesses a MPB near 50-50 composition similar to PZT system.

Presently, the polymer-matrix composites with high dielectric permittivity have also received increasing interest for various potential applications such as underwater acoustic transducers, medical diagnostic transducers, and high frequency and energy harvesting applications [12–16]. As a result, a wide variety of high dielectric constant composite materials have been developed. Efforts to improve the overall dielectric performance of these materials have been devoted to maximize the dielectric constant and suppress the dielectric loss. Generally, $BaTiO_3$/(BT), $BaSrTiO_3$/(BST), BNBT, and KNN based ceramics have been actively explored as fillers [17–20]. The ceramic-polymer composites combine the properties of polymers such as mechanical flexibility, high strength, design flexibility, formability, and low cost with the high electroactive functional properties of ceramic materials. The advantages of these composites are higher dielectric constant with low dielectric loss, high electromechanical

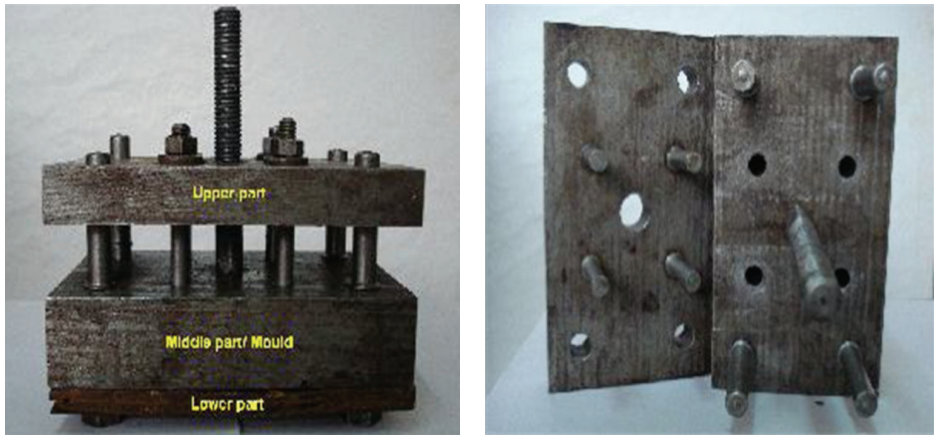

(a) (b)

Figure 1: Steel moulds designed for the preparation of cylindrical (pin) type specimens.

coupling coefficient (k_t), and lower acoustic impedance (Z_0). Ceramic-polymer composites in different volume fractions with different connectivity patterns have been designed and fabricated for improving dielectric, piezoelectric, and pyroelectric properties [21, 22]. According to the connectivity pattern between the ceramic and polymer phases, ceramic-polymer composites can be classified into 10 different types. Among these 10 types, the 3-3, 1-3, and 0-3 connectivity (particles connected in 3 dimensions) patterns of composites are extensively studied [23–25]. The ceramic-polymer composites with 0-3 connectivity basically consist of separated ceramic particles randomly dispersed in the polymer matrix. Therefore, in 0-3 ceramic-polymer composites the ceramic particles are connected in zero dimensions in a three-dimensionally interconnected polymer matrix. The advantages of the 0-3 composites are that they are easy to fabricate, the volume fraction of the ceramic phase can be varied in a wide range, they have good flexibility, and they facilitate mass production. Among different polymers, epoxy resins are excellent electrical insulators and protect electrical components from short circuiting, dust, and moisture. Also epoxy resins are used in overmolded integrated circuits, transistors, and hybrid circuits and in making printed circuit boards. Flexible epoxy resins are used for potted transformers and inductors [26].

In this work, (BZT-BCT) ceramic powder with different volume fractions is incorporated into epoxy polymer matrix to form 0-3 composites. The structural, microstructural, and dielectric properties of the synthesized composites have been investigated and discussed in detail. And also, the experimental data of the dielectric constant of (BZT-BCT)-epoxy composites were fitted to several theoretical equations for prediction of the effective dielectric constant of ceramic-polymer composites.

2. Materials and Methods

Lead free (BZT-BCT) ferroelectric ceramic samples were prepared by solid state reaction route. The synthesis of (BZT-BCT) system has been reported by the author of the paper [27].

The type of epoxy resin, used in the present investigation, is Araldite-AW-106, which chemically belongs to epoxide family. Its common name is bisphenol A diglycidyl ether. 1,3-Propanediamine (HV-953-IN) has been used as hardener. The 0-3 composites were prepared by hand lay-up technique. For the fabrication of (BZT-BCT)-epoxy composites, the (BZT-BCT) powder sintered at 1400°C for 6 h was mixed with epoxy resin and hardener. For different volume fractions of ceramics, a calculated amount of epoxy resin and hardener (in the weight ratio of 15 : 1) was thoroughly mixed with gentle stirring to minimize air entrapment. A steel mould, shown in Figure 1, has been designed and fabricated in the workshop and used for the preparation of cylindrical (pin) type specimen of length ~35 mm and diameter of ~10 mm. The mixture of (BZT-BCT) ceramic powder and epoxy resin were poured into the cylindrical cavity of the mould, which was fixed properly. During fixing some of the mixture may squeeze out, which requires proper care. After closing the mould the specimens were allowed to solidify in the mould at the RT for 24 h. A series of (BZT-BCT)-epoxy composites with different ceramic volume fractions ranging from 5% to 25% were fabricated. For the purpose of comparison, the matrix material was also cast under similar condition. After curing, the cylindrical samples were taken out from the mould and cut into required shapes and sizes for different measurements and characterizations.

XRD analyses of the ceramics and composites were performed on a Philips X-ray diffractometer X'Pert MPD using Cu K_α(λ = 0.15405 nm) radiation in order to examine the phases present in the system. The microstructures were observed using a JEOL JSM-6480LV scanning electron microscope (SEM). The bulk densities of the samples were measured by Archimedes' method. Silver paste was applied on both sides of the samples for the electrical measurements. ε_r and $\tan\delta$ were measured as a function of both temperature and frequency using a computer interfaced HIOKI 3532-50 LCR-HITESTER.

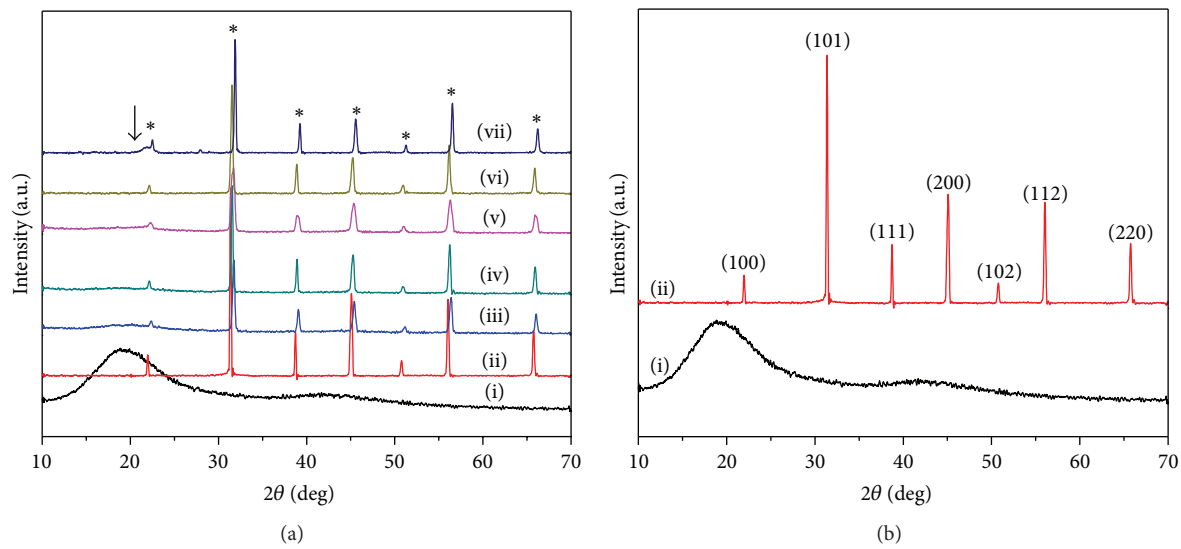

Figure 2: (a) XRD patterns of (i) sintered (BZT-BCT) ceramic, (ii) pure epoxy polymer, and (BZT-BCT)-epoxy composites with vol% (iii) 5, (iv) 10, (v) 15, (vi) 20, and (vii) 25 of ceramic fillers, where ↓ and ∗ represent epoxy and (BZT-BCT) phases, respectively. (b) XRD patterns of (i) calcined (BZT-BCT) ceramic powder and (ii) epoxy polymer.

Table 1: Structural parameters of (BZT-BCT)-epoxy composites with the variation of volume % of (BZT-BCT) ceramic fillers.

Compositions	Structure	Lattice parameters (Å)	Volume (Å^3)	Crystallite size (Å) with error	Microstrain (%)
(BZT-BCT)	Tetragonal-monoclinic	$a = 3.9963$, $c = 4.0175$ $a = 5.6452$, $b = 4.0152$, $c = 3.9943$	$V = 64.16$ $V = 64.13$	599 (105)	0.02
5 (BZT-BCT)-95epoxy composite	Tetragonal	$a = 3.9852$, $c = 4.0035$, $c/a = 1.0046$	$V = 63.58$	411 (48)	0.07
10 (BZT-BCT)-90epoxy composite	Tetragonal	$a = 3.9916$, $c = 4.0002$, $c/a = 1.0021$	$V = 63.74$	840 (147)	0.12
15 (BZT-BCT)-85epoxy composite	Tetragonal	$a = 3.9926$, $c = 4.0041$, $c/a = 1.0029$	$V = 63.83$	226 (16)	0.04
20 (BZT-BCT)-80epoxy composite	Tetragonal	$a = 4.0004$, $c = 4.0048$, $c/a = 1.0011$	$V = 64.09$	368 (27)	0.001
25 (BZT-BCT)-75epoxy composite	Tetragonal	$a = 3.9939$, $c = 4.0199$, $c/a = 1.0065$	$V = 64.12$	861 (145)	0.075

3. Results and Discussion

Figure 2(a) shows the XRD patterns of (BZT-BCT)-epoxy composites. The XRD patterns of the composites reveal the presence of both (BZT-BCT) ceramics and epoxy polymer separately, as desired in a 0-3 ceramic-polymer composite [23]. Figure 2(b) shows the XRD patterns of (BZT-BCT) calcined ceramic powder and epoxy polymer. The XRD of calcined (BZT-BCT) ceramic powder shows a typical perovskite phase without any unwanted secondary phase peaks, while epoxy turns out to be amorphous. With the increase of (BZT-BCT) ceramic powder in the (BZT-BCT)-epoxy composites, the relative intensity of amorphous phase decreases in the low 2θ angle range (20–30°). It suggests that as the content of (BZT-BCT) ceramic powder increases, the (BZT-BCT) phases start dominating the crystal properties of (BZT-BCT)-epoxy composites. The lattice parameters and the structure of (BZT-BCT)-epoxy composites are calculated using a computer program package "Powdmult" [28]. Standard deviations, S.D. = $(d_{obs} - d_{cal})$, where "d" is interplane spacing, are found to be minimum for different crystal structures. The crystallite size and microstrain are calculated using William Hall analysis by using the following formula [29]:

$$\beta \cos\theta = 4\varepsilon \sin\theta + \frac{\lambda}{D}, \tag{1}$$

where β represents the full width half maximum peak, ε gives the microstrain, λ is the wave length of the X-ray used, and D is the crystallite size. The intercept of the linear fit of (1) gives D value and the slope gives ε value. The values of lattice parameters, crystallite size, and microstrain are given in Table 1. Figure 3 shows the SEM micrographs of pure (BZT-BCT) ceramic sintered at 1400°C for 6 h and (BZT-BCT)-epoxy composites with different volume % of ceramic powder. The (BZT-BCT) ceramic sample exhibits regular shaped grains with clear grain boundaries and less porosity with an average grain size of ~7.76 μm. The black region is the epoxy and the white and gray particles are the sintered (BZT-BCT) ceramic powders. It can be seen that the (BZT-BCT) particle distribution is homogeneous with small agglomeration. The ceramic powder is evenly distributed and surrounded by epoxy matrix, which clearly indicates 0-3 type of connectivity [23]. Uniform distribution increases with the

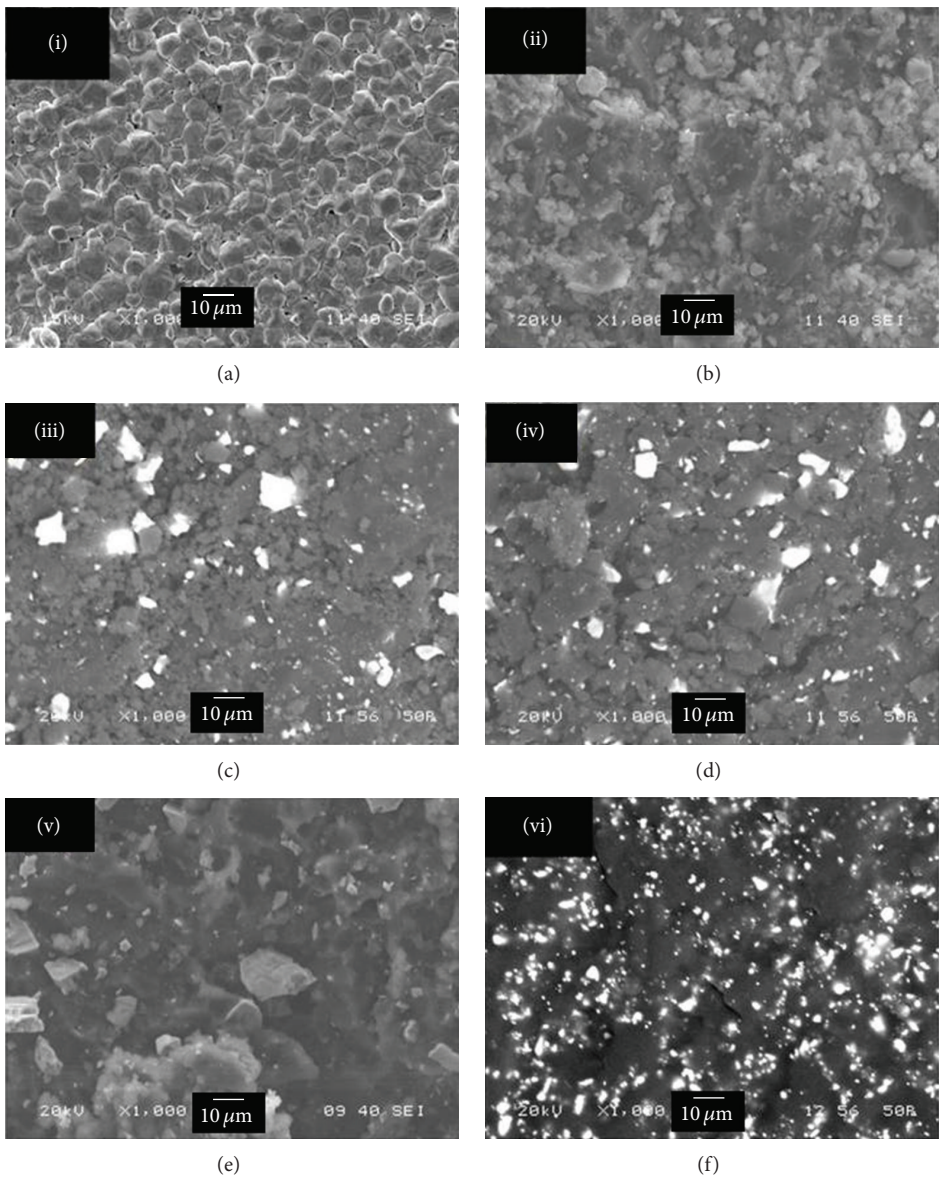

Figure 3: SEM micrograph of (i) sintered (BZT-BCT) ceramic and (BZT-BCT)-epoxy composites with the vol % (ii) 5, (iii) 10, (iv) 15, (v) 20, and (vi) 25 of ceramic fillers.

increase in (BZT-BCT) ceramic volume % in the polymer matrix. The values of density and porosity of composite samples are listed in Table 2. The density of the composite samples is found to increase from 1.29 to 1.73 g/cm^3 with the increase of volume % of (BZT-BCT) powder from 5 to 20 in (BZT-BCT)-epoxy composites. But the density decreases for the 25% volume fraction of (BZT-BCT) powder in (BZT-BCT)-epoxy composites, which can be attributed to the limit of addition of ceramic powder in the composite.

The frequency dependence of both ε_r and $\tan\delta$ of sintered (BZT-BCT) ceramic samples has already been reported in our paper [27]. Figure 4(a) shows the variation of ε_r with frequency for the (BZT-BCT)-epoxy composite samples. Good dispersion along with homogeneous packing of ceramic filler is likely to exhibit high dielectric constant [30]. A maximum value of $\varepsilon_r \sim 34$ at 1 kHz frequency is achieved for the 20 vol.% of (BZT-BCT) ceramic filler in the composites and beyond 20% ε_r value starts decreasing. As expected, in all the cases, the effective dielectric constants obtained are higher than that of pure epoxy but much lower than that of pure (BZT-BCT) ceramics. The increase in ε_r values of composites up to 20% of filler can be related to the increase in density and also increase in connectivity between ceramics [21]. The decrease of ε_r in case of 25 vol% of the (BZT-BCT) ceramics in (BZT-BCT)-epoxy composites may be attributed to the decrease in density and increase in porosity of the composite. In all the (BZT-BCT)-epoxy composite samples, with the increase in frequency, ε_r decreases very fast up to 10^4 Hz, and in the frequency range from 10^4 to 10^6 Hz, it is almost constant. This can be related to the intermolecular cooperative motions and hindered dielectric rotations in the composite samples [31].

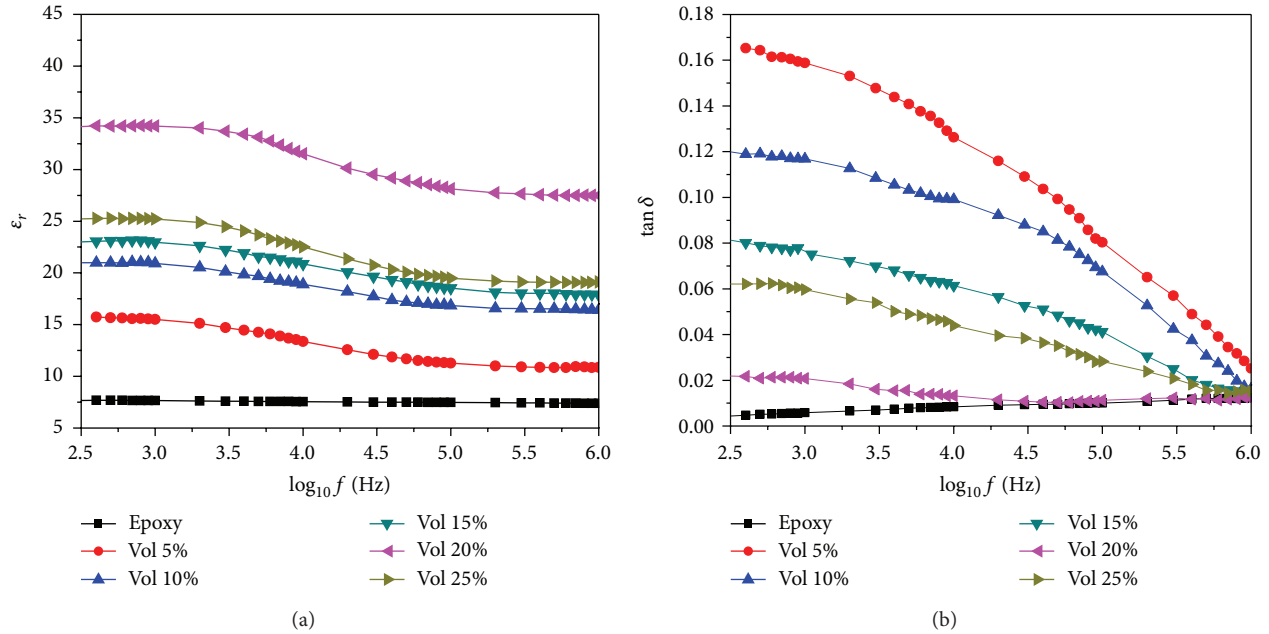

FIGURE 4: Frequency dependence of (a) ε_r and (b) $\tan\delta$ of (BZT-BCT)-epoxy composite samples.

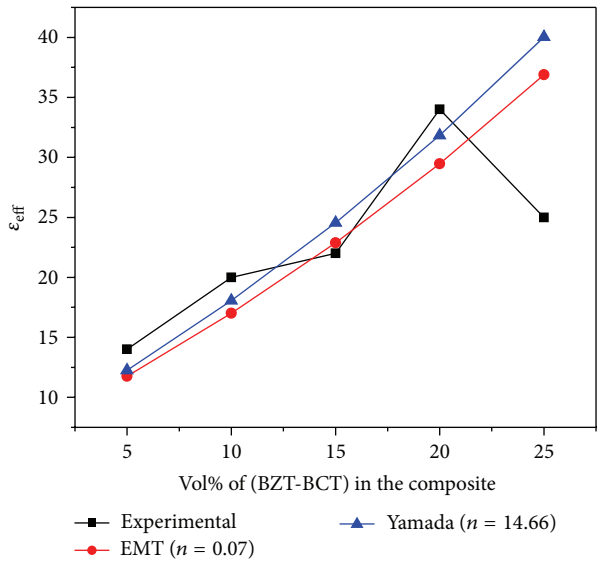

FIGURE 5: Variation of effective dielectric constant (ε_{eff}) (measured at RT and 1 kHz frequency) of (BZT-BCT)-epoxy composites as a function of volume % of (BZT-BCT) ceramics.

Figure 4(b) shows the variation of $\tan\delta$ versus frequency for the composite samples. Dielectric loss decreases with the increase in frequency for all the compositions and becomes almost constant in the higher frequency range. The decrease in dielectric loss with frequency can be due to the decrease of space charge polarization [32]. The decrease in tanδ with frequency can also be ascribed to the decrease in electrical conductivity of the composites with the increase in frequency [33]. The $\tan\delta$ also decreases with the increase in ceramic loading in the (BZT-BCT)-epoxy composites, but, with 25 vol% of ceramic filler in the composite, the $\tan\delta$ value again increases. This can be explained in terms of percolation threshold [34]. It is known that percolation threshold varies depending upon the matrix, filler, particle size, shapes, spatial orientation, and processing parameters. In case of (BZT-BCT)-epoxy composites, the percolation limit of the composite (in terms of BZT-BCT ceramic particles) may have reached 20 vol%. ε_r and $\tan\delta$ values at RT and 1 kHz frequency of the composite samples are given in Table 2.

Various dielectric models are used in order to predict the effective dielectric constant (ε_{eff}) of the (BZT-BCT)-epoxy composites. Figure 5 shows the comparison of the RT ε_r

Table 2: Different parameters of (BZT-BCT)-epoxy composites with the variation of volume % of (BZT-BCT) ceramic fillers.

Properties	Materials						
	(BZT-BCT) 50/50	Epoxy	(BZT-BCT)-epoxy composites with different vol % of (BZT-BCT) ceramics				
			5	10	15	20	25
ε_r at RT at 1 kHz	3800	7	14	20	22	34	25
Tan δ at RT at 1 kHz	0.01	0.0052	0.1587	0.1169	0.0756	0.0195	0.0596
$\varepsilon_{r\,\max}$ at 1 kHz	5500		18.62	24.16	29.07	44.97	29.34
$T_{\max}$ corresponding to $\varepsilon_{r\,\max}$ at 1 kHz	108		123	133	148	142	150
Density (g/cm^3)	5.7	1.74	1.29	1.45	1.63	1.73	1.62
Apparent porosity of the composite in %			1.22	0.96	0.88	1.73	1.02

values of the composites at 1 kHz (experimental), for different volume % of (BZT-BCT), with the ε_r values,calculated based on various models.

For the (BZT-BCT)-epoxy composites, the most commonly used dielectric mixing models, the Lichtenecker model [35], Maxwell's model [36], and the Clausius-Mossotti model [37], are not fitting properly.

Effective medium theory (EMT) [38] model is used for calculating the ε_{eff} of the composites.

According to EMT model the ε_{eff} is given by

$$\varepsilon_{\text{eff}} = \varepsilon_p \left[1 + \frac{f_c \left(\varepsilon_c - \varepsilon_p \right)}{\varepsilon_p + n \left(1 - f_c \right) \left(\varepsilon_c - \varepsilon_p \right)} \right], \tag{2}$$

where f_c is the volume fraction of the ceramic powder ε_c, ε_p, and n are the dielectric constants of the ceramic particle, polymer and the ceramic morphology fitting factor, respectively. n takes the values 0 (prolate), 1/3 (sphere), and 1(oblate) and intermediate values for intermediate shapes [38].

The parameter n is calculated by using (2) to fit the experimental and theoretical values of the (BZT-BCT)-epoxy composites. The calculated ε_{eff} values are given in Table 3. The experimental ε_r values fit well into the EMT model with $n = 0.07$ for the volume fractions (≤20%) of the (BZT-BCT) ceramics.

The model, developed by Thomas et al. [36], is also used to predict ε_{eff} of the presently studied composites. As per this model,

$$\varepsilon_{\text{eff}} = \varepsilon_1 \left[1 + \frac{n f_{(\text{BZT-BCT})} \left(\varepsilon_2 - \varepsilon_1 \right)}{n\varepsilon_1 + \left(\varepsilon_2 - \varepsilon_1 \right) \left(1 - f_{(\text{BZT-BCT})} \right)} \right]. \tag{3}$$

Here ε_1 and ε_2 are the ε_r values of the epoxy and (BZT-BCT) ceramics, respectively. n is the parameter related to the geometry of the ceramic particles and $f_{(\text{BZT-BCT})}$ is the volume fraction of the (BZT-BCT) ceramics in the matrix phase. The parameter n is evaluated such that the mismatch between the theoretical and observed values is minimum. The experimental results are comparable to those obtained using this model for the volume fractions up to 20% of the (BZT-BCT) ceramics, when the parameter n is ~14.66 (given in Table 3).

The temperature dependence of both ε_r and tan δ for the sintered (BZT-BCT) ceramic samples has been reported earlier by the same authors [27]. Figure 6(a) shows the temperature dependence of ε_r at 1 kHz frequency for the (BZT-BCT)-epoxy composite samples. The increase in values of ε_r from RT to 60°C range is very small, suggesting the low value of temperature coefficient of capacitance. ε_r value increases continuously to a certain temperature ($T_{\max}$) corresponding to $\varepsilon_{r\,\max}$ for the composite samples. With the increase in vol% of ceramic filler in the composites, the effect of ceramic starts appearing and there starts dependence of T_c or $T_{\max}$ on the ceramic content. There is no systematic variation of $T_{\max}$ (shown in Table 2) corresponding to $\varepsilon_{r\,\max}$ at 1 kHz for the composites. This can be ascribed to the mobility of polymers, the disruption of contacts between the filler particles caused by the thermal expansion of the matrix and ceramic, and the change in the dielectric response of the ceramic particles with temperature [39].

Figure 6(b) shows the temperature dependence of tan δ of the (BZT-BCT)-epoxy composite samples at 1 kHz frequency. There is a decrease in tan δ with the increase in volume % (up to 15) of (BZT-BCT) ceramic filler content in (BZT-BCT)-epoxy composite samples. The tan δ values sharply decrease attaining minima in the temperature range 110–150°C and then suddenly increase with increasing temperature. The dielectric properties of polymers depend upon the charge distribution and the thermal motion of the polar groups. The minima in the dielectric loss curves correspond to the glass transition regions (T_g) of the polymer. On further increase in temperature, the thermal oscillation intensifies and the degree of order of orientation diminishes showing the sudden increase in loss curves [29].

However, the (BZT-BCT) ceramic content has been restricted to 25 vol% in the (BZT-BCT)-epoxy composites. This may be due to the fact that when the volume fraction of the ceramic filler is ~30%, the flexibility of a specimen becomes too weak to be used in flexible devices. Again the density and dielectric constant start decreasing beyond 20% of (BZT-BCT) in the composite samples. A high dielectric constant at RT and a low temperature coefficient of capacitance from RT to 60°C make the 20 vol% ceramic filled (BZT-BCT)-epoxy composite suitable for flexible capacitors devices.

Table 3: Comparison of experimental and theoretical values of ε_{eff} of (BZT-BCT)-epoxy composites with the variation of volume % of (BZT-BCT) ceramic fillers.

Vol % of (BZT-BCT) ceramic fillers in (BZT-BCT)-epoxy composites	Experimental values of ε_r (at 1 kHz and at RT)	Theoretical values of ε_r (at 1 kHz and at RT) according to different models	
		EMT model	Yamada model
5	14	11.75	12.25
10	20	17.01	18.07
15	22	22.88	24.56
20	34	29.46	31.82
25	25	36.89	40.03

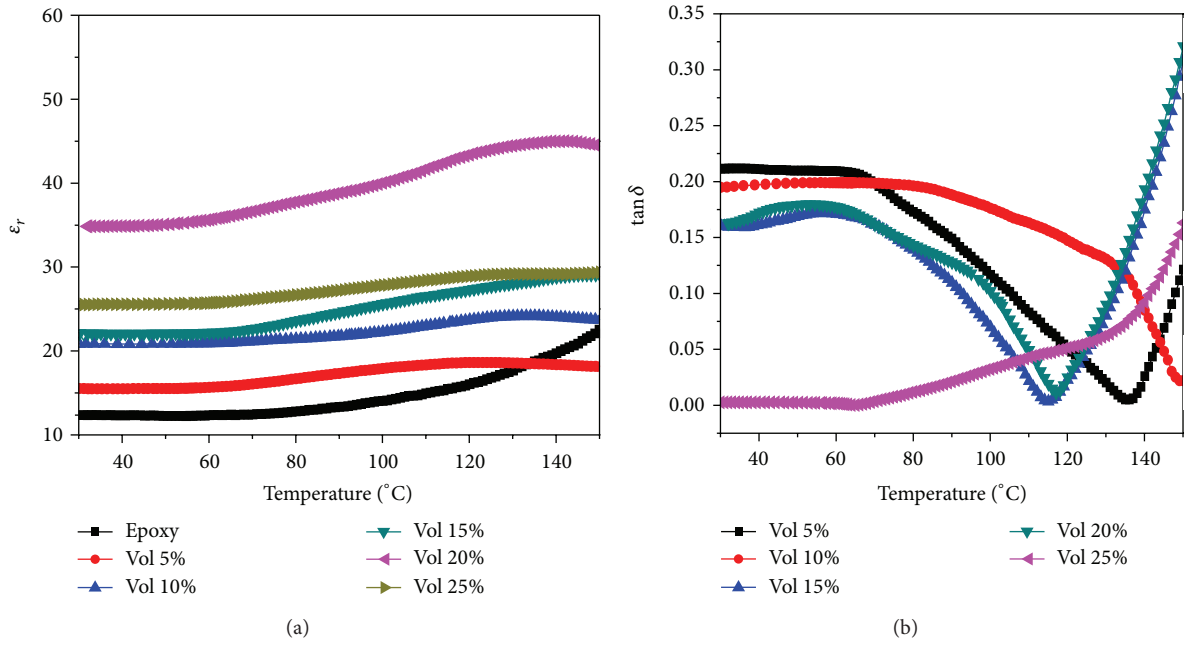

Figure 6: Temperature dependence of (a) ε_r of (BZT-BCT)-epoxy composites and (b) $\tan\delta$ of (BZT-BCT)-epoxy composite samples.

4. Conclusions

Φ(BZT-BCT)-(1−Φ) epoxy composites with vol% of (BZT-BCT) ceramics ranging from 5% to 25% were fabricated and characterized. The XRD patterns of the composite specimens showed the presence of peaks corresponding to both epoxy polymer and (BZT-BCT) ceramics separately, as desired in a 0-3 ceramic-polymer composite. The density of the composite samples is found to increase from 1.29 to 1.73 g/cm^3 with the increase of volume fraction of (BZT-BCT) in (BZT-BCT)-epoxy composites. From SEM study, the (BZT-BCT) ceramic powders were found to be well dispersed in the epoxy polymer matrix. The oscillatory behavior of $\tan\delta$ with frequency was attributed to some relaxation processes, which usually occur in heterogeneous system. Finally, 0.2(BZT-BCT)-0.8(epoxy) composite showed the highest relative permittivity (ε_r) ~ 34 with low temperature coefficient of capacitance and suggested that it can be suitable for flexible capacitors devices.

References

[1] M. R. Soares, A. M. R. Senos, and P. Q. Mantas, "Phase coexistence region and dielectric properties of PZT ceramics," *Journal of the European Ceramic Society*, vol. 20, no. 3, pp. 321–334, 2000.

[2] P. Kumar, S. Sharma, O. P. Thakur, C. Prakash, and T. C. Goel, "Dielectric, piezoelectric and pyroelectric properties of PMN-PT (68:32) system," *Ceramics International*, vol. 30, no. 4, pp. 585–589, 2004.

[3] B. K. Gan and K. Yao, "Structure and enhanced properties of perovskite ferroelectric PNN-PZN-PMN-PZ-PT ceramics by Ni and Mg doping," *Ceramics International*, vol. 35, no. 5, pp. 2061–2067, 2009.

[4] M. Roth, E. Dul'In, E. Mojaev, and M. Tseitlin, "Characterization of lead-based relaxor ferroelectric crystals by acoustic emission," *Optical Materials*, vol. 34, no. 2, pp. 381–385, 2011.

[5] D. Zhou, Y. Tang, F. Wang et al., "Improved dielectric and electrical insulating properties in $Pb(Mg_{1/3}Nb_{2/3})_{0.62}Ti_{0.38}O_3$ based multilayer ferroelectric thin films," *Thin Solid Films*, vol. 522, pp. 457–462, 2012.

[6] R. Zuo and C. Ye, "Structures and piezoelectric properties of $(NaKLi)_{1-x}(BiNaBa)_xNb_{1-x}Ti_xO_3$ lead-free ceramics," *Applied Physics Letters*, vol. 91, no. 6, Article ID 062916, pp. 1–3, 2007.

[7] K. Kurihara and M. Kondo, "High-strain piezoelectric ceramics and applications to actuators," *Ceramics International*, vol. 34, no. 4, pp. 695–699, 2008.

[8] W. Wanga, S. W. Or, Q. Yuea et al., "Ternary piezoelectric single-crystal PIMNT based 2-2 composite for ultrasonic transducer applications," *Sensors and Actuators A*, vol. 196, pp. 70–77, 2013.

[9] I. Payo and J. M. Hale, "Sensitivity analysis of piezoelectric paint sensors made up of PZT ceramic powder and water-based acrylic polymer," *Sensors and Actuators A*, vol. 168, no. 1, pp. 77–89, 2011.

[10] S. H. Choy, W. K. Li, H. K. Li, K. H. Lam, and H. L. W. Chan, "Study of BNKLBT-1.5 lead-free ceramic/epoxy 1-3 composites," *Journal of Applied Physics*, vol. 102, no. 11, Article ID 114111, 2007.

[11] W. Liu and X. Ren, "Large piezoelectric effect in pb-free ceramics," *Physical Review Letters*, vol. 103, Article ID 257602, pp. 1–4, 2009.

[12] D. Zhou, K. H. Lama, Y. Chena et al., "Lead-free piezoelectric single crystal based 1-3 composites for ultrasonic transducer applications," *Sensors and Actuators A*, vol. 182, pp. 95–100, 2012.

[13] K. H. Lam, H. F. Ji, F. Zheng, W. Ren, Q. Zhou, and K. K. Shung, "Development of lead-free single-element ultrahigh frequency (170-320 MHz) ultrasonic transducers," *Ultrasonics*, vol. 53, pp. 1033–1038, 2013.

[14] B. Jadidian, N. Hagh, A. Winder, and A. Safari, "25 MHz ultrasonic transducers with lead- free piezoceramic, 1-3 PZT fiber-epoxy composite, and PVDF polymer active elements," *IEEE Transactions on Ultrasonics, Ferroelectrics, and Frequency Control*, vol. 56, no. 2, pp. 368–378, 2009.

[15] S. George and M. T. Sebastian, "Three-phase polymer-ceramic-metal composite for embedded capacitor applications," *Composites Science and Technology*, vol. 69, no. 7-8, pp. 1298–1302, 2009.

[16] M. Aureli, C. Prince, M. Porfiri, and S. D. Peterson, "Energy harvesting from base excitation of ionic polymer metal composites in fluid environments," *Smart Materials and Structures*, vol. 19, no. 1, Article ID 015003, 2010.

[17] K.-C. Cheng, C.-M. Lin, S.-F. Wang, S.-T. Lin, and C.-F. Yang, "Dielectric properties of epoxy resin-barium titanate composites at high frequency," *Materials Letters*, vol. 61, no. 3, pp. 757–760, 2007.

[18] T. Hu, J. Juuti, H. Jantunen, and T. Vilkman, "Dielectric properties of BST/polymer composite," *Journal of the European Ceramic Society*, vol. 27, no. 13–15, pp. 3997–4001, 2007.

[19] D.-Y. Wang and H. L.-W. Chan, "A dual frequency ultrasonic transducer based on BNBT-6/epoxy 1-3 composite," *Materials Science and Engineering B*, vol. 99, no. 1–3, pp. 147–150, 2003.

[20] Y. Zhen, J.-F. Li, and K. Wang, "Fabrication and electrical properties of fine-scale 1-3 piezoceramic/epoxy composites using $(K,Na)NbO_3$-based lead-free ceramics," *Ferroelectrics*, vol. 358, no. 1, pp. 161–168, 2007.

[21] G. Zhang and M. S. Wu, "Connectivity and shape effects on the effective properties of piezoelectric-polymeric composites," *International Journal of Engineering Science*, vol. 48, no. 1, pp. 37–51, 2010.

[22] M. T. Sebastian and H. Jantunen, "Polymer-ceramic composites of 0-3 connectivity for circuits in electronics: a review," *International Journal of Applied Ceramic Technology*, vol. 7, no. 4, pp. 415–434, 2010.

[23] D. T. Le, N. B. Do, D. U. Kim, I. Hong, I.-W. Kim, and J. S. Lee, "Preparation and characterization of lead-free $(K_{0.47}Na_{0.51}Li_{0.02})(Nb_{0.8}Ta_{0.2})O_3$ piezoceramic/epoxy composites with 0-3 connectivity," *Ceramics International*, vol. 38, no. 1, pp. S259–S262, 2012.

[24] Y. J. Choi, M.-J. Yoo, H.-W. Kang, H.-G. Lee, S. H. Han, and S. Nahm, "Dielectric and piezoelectric properties of ceramic-polymer composites with 0-3 connectivity type," *Journal of Electroceramics*, vol. 30, no. 1-2, pp. 30–35, 2013.

[25] C. R. Bowen and V. Y. Topolov, "Piezoelectric sensitivity of $PbTiO_3$-based ceramic/polymer composites with 0-3 and 3-3 connectivity," *Acta Materialia*, vol. 51, no. 17, pp. 4965–4976, 2003.

[26] L. A. Ramajo, A. A. Cristóbal, P. M. Botta, J. M. Porto López, M. M. Reboredo, and M. S. Castro, "Dielectric and magnetic response of Fe_3O_4/epoxy composites," *Composites A*, vol. 40, no. 4, pp. 388–393, 2009.

[27] P. Mishra, Sonia, and P. Kumar, "Effect of sintering temperature on dielectric, piezoelectric and ferroelectric properties of BZT-BCT 50/50 ceramics," *Journal of Alloys and Compounds*, vol. 545, pp. 210–215, 2012.

[28] E. Wu, "POWD, an interactive powder diffraction data interpretation and indexing program ver. 2. 1," Tech. Rep., School of Physical Science, Finder's University of South Australia, Bedford Park, Australia.

[29] G. K. Williamson and W. H. Hall, "X-ray line broadening from filed Aluminium & wolfram," *Acta Metallurgica*, vol. 1, no. 1, pp. 22–31, 1953.

[30] B. Hilczer, J. Kulek, M. Polomska, M. Kosec, B. Malic, and L. Kepinski, "Dielectric relaxation in $K_{0.5}Na_{0.5}NbO_3$-PVDF composites," *Ferroelectrics*, vol. 338, pp. 159–170, 2006.

[31] C. V. Chanmal and J. P. Jog, "Dielectric relaxations in PVDF/$BaTiO_3$ nanocomposites," *Express Polymer Letters*, vol. 2, no. 4, pp. 294–301, 2008.

[32] C. Basavaraja, Y. M. Choi, H. T. Park et al., "Preparation, characterization and low frequency a.c. conduction of polypyrrole-lead titanate composites," *Bulletin of the Korean Chemical Society*, vol. 28, no. 7, pp. 1104–1108, 2007.

[33] R. Gregorio Jr. and E. M. Ueno, "Effect of crystalline phase, orientation and temperature on the dielectric properties of poly (vinylidene fluoride) (PVDF)," *Journal of Materials Science*, vol. 34, no. 18, pp. 4489–4500, 1999.

[34] K. Osińska, A. Lisińska-Czekaj, H. Bernard, J. Dzik, M. Adamczyk, and D. Czekaj, "Dielectric properties of bismuth ferrite—bismuth titanate ceramic composite," *Archives of Metallurgy and Materials*, vol. 56, no. 4, pp. 1093–1104, 2011.

[35] A. V. Goncharenko, V. Z. Lozovski, and E. F. Venger, "Lichtenecker's equation: applicability and limitations," *Optics Communications*, vol. 174, no. 1–4, pp. 19–32, 2000.

[36] P. Thomas, K. T. Varughese, K. Dwarakanath, and K. B. R. Varma, "Dielectric properties of Poly(vinylidene fluoride)/$CaCu_3Ti_4O_{12}$ composites," *Composites Science and Technology*, vol. 70, no. 3, pp. 539–545, 2010.

[37] M. Dinulović and B. Rašuo, "Dielectric modeling of multiphase composites," *Composite Structures*, vol. 93, no. 12, pp. 3209–3215, 2011.

[38] H. Zewdie, "Effective medium theory of the mechanical, dielectric and piezoelectric properties of ferroelectric

ceramic-polymer composite," *Bulletin of the Chemical Society of Ethiopia*, vol. 12, no. 2, pp. 159–171, 1998.

[39] L. Ramajo, M. Reboredo, and M. Castro, "Dielectric response and relaxation phenomena in composites of epoxy resin with $BaTiO_3$ particles," *Composites A*, vol. 36, no. 9, pp. 1267–1274, 2005.